Supplementary material

1. Supplementary Materials and Methods

ATM Immunohistochemistry: ATM protein expression was determined by immunohistochemistry (IHC) on 3 to 4-μM-thick formalin-fixed, paraffin-embedded (FFPE) sections using a rabbit monoclonal anti-ATM antibody, clone Y170 (catalogue no. ab32420; Abcam plc, Cambridge, UK), as previously described (Sundar, Miranda et al. 2018). Briefly, antigen unmasking was performed by heating slides in high pH buffer solution, in a Menapath Antigen Access Unit and, subsequently, antibody incubation and detection were performed using an i6000 Biogenex Autostainer (Launch Diagnostics, Longfield, England). All IHC slides were evaluated by a pathologist, blinded to any other clinical or molecular data, for nuclear staining intensity of ATM and semi-quantitatively classified using the H-score formula and, subsequently, were scanned at high resolution (200x) using the ZEISS Axio Scan.Z1 digital slide scanner (Carl Zeiss AG, Oberkochen, Germany). A supervised machine learning algorithm (HALO AI, Indica Labs, New Mexico, USA) was trained to recognize prostate cancer foci and fibromuscular prostate stroma. Colour deconvolution for DAB and haematoxylin stains was performed. Finally, cell recognition and nuclear segmentation was optimized for neoplastic cells, and recognition of nuclear ATM staining was optimized. The analysis algorithm was adjusted to provide continuous data on the intensity of nuclear ATM in the automatically annotated tumour regions. The sum of optical densities (OD) was then divided by the calculated area, providing an average staining score for each case. This IHC assay was initially validated by comparing the detection of ATM protein expression in VCaP, GM-012526 and DU145 whole cell lysates. To confirm specificity, DU145 cells were transfected with either non-targeting control siRNA or ON-TARGETplus pooled ATM siRNA

(Dharmacon; GE Healthcare: Chicago, Illinois, United States), and analysed 72-hours after transfection. GM-01526 was used as a negative control.

NGS assays in patient biopsies: Genomic DNA was isolated from 6x10µm FFPE tissue sections using the QIAmp DNA FFPE Tissue kit (Qiagen). Samples presenting less than 50% tumour content were microdissected prior to DNA extraction. DNA was quantified with the Quant-iT high-sensitivity PicoGreen double-stranded DNA Assay Kit (Invitrogen). Quality controls were implemented using the Illumina FFPE QC kit (WG-321-1001) as previously described (Mateo et al, JCI 2020).

Libraries for targeted sequencing were constructed as described previously (Mateo et al., NEJM, 2015; Mateo et al, JCI 2020). In brief, 40ng of DNA from each sample were used to construct libraries using a customized panel (Generead DNAseq Mix-n-Match Panel v2; Qiagen) covering 113 genes and run in a MiSeq Sequencer (Illumina). FASTQ files were generated using the Illumina MiSeq Reporter v2.5.1.3. Sequence alignment and mutation calling was performed using BWA tools and the GATK variant annotator by the Qiagen GeneRead Targeted Exon Enrichment Panel Data Analysis Portal. Copy number variations (CNV) were assessed using CNVkit (v0.3.5, https://github.com/etal/cnvkit) as previously reported (Seed et al, CCR 2017).

Whole-exome sequencing was performed using Kapa Hyper Plus Library Prep Kits and the Agilent SureSelectXT V6 target enrichment kit. Paired-end sequencing was performed using the NovaSeq 6000 S2 flow cell (2x100 cycles, Illumina). FASTQ files were generated from the sequencer's output using Illumina bcl2fastq2 software (v.2.17.1.14, Illumina), with the default chastity filter to select sequence reads for subsequent analyses. All sequencing reads were aligned to the human genome reference sequence (GRCh37-hg19) using the BWA-MEM algorithm (v. 0.7.12), with indels being

realigned using the Stampy (v.1.0.28) package. Picard tools (v.2.1.0) were used to remove PCR duplicates and to calculate sequencing metrics for quality control check. The Genome Analysis Toolkit (GATK, v. 3.5-0) was applied to realign local indels, recalibrate base scores, and identify point mutations and small insertions and deletions. Somatic point mutations and indels were called using MuTect2 by comparing tumour DNA to germline DNA control, and copy-number estimation was obtained through the modified ASCAT2 package

Clinical and demographics data collection and analyses: Demographic and clinical data for each patient were retrospectively collected from the hospital electronic patient records under local IRB approval reference 04/Q0801/60.

The ATM loss cohort was defined as those patients in the study population with complete loss of ATM by IHC (H score of 0), for whom NGS data were also available (n=61). Demographic and tumour baseline data, including date of diagnosis, date of metastasis and castration-resistance, were collected, as well as time on therapy and date of death or last follow-up.

In order to have a contemporaneous control group, we compared the clinical data to a cohort of patients from a previously published study (n=60) with all patients having an ATM-H score>50. Clinical outcomes were overall survival from diagnosis of PC, and from diagnosis of CRPC, respectively, time from diagnosis of PC to CRPC, and time on novel hormonal therapy (either abiraterone or enzalutamide). Time-to-event analyses of these outcomes included the Kaplan-Meier estimator for visualization of survival, and to determine median survival time. Additionally, hazard ratios with 95% confidence intervals obtained by Cox regression and the log-rank test were used to assess differences

between the ATM loss group and the control group. All clinical data were analysed using R (Version 3.6.2)

Immunofluorescence. Cells were seeded in 96-well plates (4000/well) and treated with the drug(s) of interest, or vehicle, for 24-hours. After a first wash in PBS, cells were washed for 5 minutes in PBS containing 0.1% of Tween-20 (PBST) and fixed in 2% paraformaldehyde (PFA) for 30-minutes. For RAD51 staining, a pre-extraction step using CSK buffer (25 mM HEPES, pH 7.4, 50 mM NaCl, 3 mM MgCl2, 300 mM sucrose, and 0.5% Triton X-100)[1] for 4-minutes on ice was implemented prior to fixation. Cell were then washed for 5-minutes in PBS and permeabilized with PBS Triton-X5 (0.2%) for 5-minutes. After blocking in PBST-BSA5% for 1-hour, cells were incubated with the primary antibody of interest. Following 1-hour incubation of primary antibody at RT, fixed cells were washed and incubated with the corresponding ALEXA secondary antibodies in PBST containing 5% BSA for 30-minutes. To remove the secondary antibody, cells were washed x1 time in PBST, and x2 times for 5-minutes in PBS, and stained with DAPI.Image acquisition was performed using an automated high-throughput microscope (IN Cell Analyzer 2000, GE Healthcare) with a 40x objective. Multiple fields within a well were acquired in order to include a minimum of 1,000 cells per sample-well. High content analysis (HCA) of the images was processed using the IN Cell Investigator 2.7.3 software as described previously (Herranz et al., 2015). The nuclei were segmented using Top-Hat segmentation, specifying a minimum nucleus area of 100 μm^2. Nuclear IF in the reference wavelength, i.e. all the other wavelengths apart from DAPI, was quantitated as an average of pixel intensity (grey scale) within the specified nuclear area. Rad51, yH2AX and 53BP1 foci were quantified as number [n] of foci per nucleus.

Western Blot. Cells were lysed in RIPA buffer (50mM Tris pH8, 150 mM NaCl, 1% Triton, 0,5% Na-Deoxycholate, 0.1% SDS, 1mM EDTA) supplemented with 1 tablet of PhosStop and 1 tablet of protease inhibitors per 10 ml RIPA. Lysates were kept on ice for 30-minutes, sonicated for 15-seconds, and cleared by centrifugation. PDX lysate was obtained by mechanical homogenization, reconstituted in RIPA buffer. Protein extracts (25 µg) were separated on 4-12% NuPAGE® Bis-Tris gel (Invitrogen) by electrophoresis and subsequently transferred onto Immobilon-PTM PVDF membranes of 0.45 µm pore size (Millipore). Membranes were incubated with red ponceau and blocked in blocking buffer (5X milk TSBT/ 5X BSA TSBT) for 1 hour. Primary antibody was incubated overnight at 4ºC, and the membrane was then washed 6-times for 5-minutes in TSBT. After 1-hour of incubation with the secondary antibody, the membrane was washed 6-times for 5-minutes. For the 22Rv1 CRISPR clones, lysis was performed on ice for 15 -minutes followed, by centrifugation at 15,000 rpm at 4°C for 15-minutes to collect protein extracts; 30ug of protein was incubated with Laemmli buffer 5x at 96ºC for 5-minutes and loaded onto an acrylamide gel. Chemiluminescence was detected using Clarity ECL Western blot detection substrate and visualized on the ChemidocTM Touch imaging system (both Bio-Rad) for cell lines and PDX lysates, or after incubation of the membrane in Pierce^{TM} ECL Plus Western Blotting Substrate and visualized on the Amersham Imagen 600 (GE) machine (22Rv.1 CRISPR clones).

Patient-derived xenograft (PDX): The generation of the CP50C ATM loss patient-derived model has been previously described (Welti et al., 2018). For the drug testing experiments, tumours were cut and subcutaneously implanted into the flank of NSG NOD scid gamma mice. Tumours were measured twice-weekly using calipers, and randomized into 7 treatment arms with 8 animals each as soon as the tumours reached a volume of

200 mm^3; body weight was monitored twice-weekly. The ATR inhibitor (BAY 1895344 in PEG400/EtOH/Water (60:10:30)) was given orally (10, 30, 50 mg/kg 2QD, - days on, 4- days off). The PARP inhibitor Olaparib (50 mg/kg) was given by intraperitoneal injection, QD in 10% 2-HPbCD/PBS. Animals were sacrificed by heart punctuation under general anaesthesia either as soon as the tumour volume exceeded a volume of 1250 mm^3 or after 8 weeks of treatment (56 days). Serum PSA was measured using the human PSA ELISA Kit (Abcam, ab264615). Tumours were taken, weighted and fixed in formalin overnight and IHC for Ki67 was performed and scored by a trained pathologist (BG) to access impact on tumour growth. Data were analyzed students t-tests (growth) or ordinary one-way ANOVA using GraphPad PRISM software. All experimental protocols were monitored and approved by The Institute of Cancer Research Animal Welfare and Ethical Review Body, in compliance with guidelines specified by the UK Home Office Animals (Scientific Procedures) Act 1986 and the United Kingdom National Cancer Research Institute guidelines for the welfare of animals in cancer research (Kilkenny et al., 2010; Workman et al., 2010).

Organoid culture (PDOs): PDX-derived organoids were cultured using a method adapted from that published by Drost et al., 2016[2], with minor alterations. Briefly PDX tumours were harvested in PDX harvesting solution (adDMEM/F12 containing 10 μM ROCK inhibitor Y27632 (Selleck Chemicals), penicillin/streptomycin, 10 mM Hepes and GlutaMAX 100× diluted all purchased form Thermofisher), cut into small pieces (< 5 qmm) and single cell suspensions were generated by mechanical separation (40 μm Corning cell strainer, Sigma Aldrich). Pellets were washed once onice-cold PBS/10 μM Y27632, and red blood cells were removed using red blood cell lysis buffer (0.8% NH4Cl in 0.1 mM EDTA in water, buffered with KHCO3 to pH of 7.2 - 7.6, incubated 1-minute

on ice) followed by another wash with ice cold PBS/Y27632. Single cell suspensions were either frozen for later use in BioCat BambankerTM freezing medium (Fisher Scientific) supplemented with 10 μM Y27632, or directly resuspended in ice-cold organoid growth medium (as published by Drost et al., 2016 with the following alterations: The p38 inhibitor SB202190 was replaced by the addition of 5 nM of NRG1 (Gil et al., 2020) and subsequently diluted in one volume of phenol red-free, growth factor reduced, Corning MatrigelTM (Fisher Scientific). Organoid domes (5-50 μl) were plated as previously described (Drost et al., 2016) and topped up with warm medium after solidification. Cultures were observed over 3-7 days until visible organoid formation could be observed. Immunohistochemistry was performed to confirm absence of ATM in the organoid cultures. For drug treatment, organoids were harvested in organoid harvesting solution (Amsbio), washed with medium and re-plated in the same way as described above and incubated in organoid growth medium for 6-10 days. Cell Titre Glo 3D (Promega) was used to assay growth of the organoids according to the manufacturer's instruction.

2. Supplementary Tables

Supplementary Table 1: Culture media for prostate cancer cell lines

All media components were purchased from Thermofisher

Cell Line:	Culture Media:
LNCaP	RPMI1640 +10%FCS, PenStrep, Glutamax
22Rv1	RPMI1640 +10%FCS, PenStrep, Glutamax
22Rv1 CRISPR clones	RPMI1640 +10%FCS, PenStrep, Glutamax
PC3	RPMI1640 +10%FCS, PenStrep, Glutamax
DU145	DMEM +10%FCS, PenStrep, Glutamax

Supplementary Table 2. Detailed information of the antibodies used for IF assays

Antigen	Antibody	Species	Dilution
RAD51	Cell signalling 8875S	Rabbit	IF 1:250
Geminin	Prot Tech	Rabbit	IF 1:500
γH2AX (ser139)	Milipore 05-636	Mouse	IF 1:1500
53BP1	Novus NB100-34	Rabbit	IF 1:1500
Secondary antibody			
IgG (H+L) Cross-Adsorbed Goat anti-mouse, Alexa Fluor 488, Invitrogen. Fisher Scientific 10256302			IF 1:500
IgG (H+L) Cross-Adsorbed Goat anti-Rabbit, Alexa Fluor 568, Invitrogen. Fisher Scientific 10463022			IF 1:500

Supplementary Table 3. Detailed information of the antibodies for IHC

Antigen	**Antibody**	**Species**	**Method**
AR CTD	Abcam ab52615	Rabbit	pH6 PC Envision
ARv7	RevMab RM7	Rabbit	pH8.1 tris/edta MW Envision
Total ATM	Abcam, ab32420	Rabbit	pH9 (Dako S236784-2) PC (Menap) Envision
Phospho Chk2 (Thr68)	Cell Signaling 2197	Rabbit	pH6 PC (menap) Rabbit ABC
cMYC	MP-415-CMEK (Menarini)	Rabbit	ER2 10 min Bond Polymer Refine
PTEN	Cell signaling D4-3 9188	Rabbit	ph6 MW Rabbit ABC
p53	Dako DO-7	Mouse	pH8.1 tris/edta MW Envision

Supplementary Table 4. Detailed information of the antibodies for WB

Antigen	Antibody	Species	Dilution
Phospho Chk1 (Ser345)	Cell Signaling 2348	Rabbit	1:1000
Phospho Chk2 (Thr68)	Cell Signaling 2197	Rabbit	1:1000
Total Chk1	Cell Signalling 2360	Mouse	1:1000
Total Chk2	Cell Signalling 3440	Mouse	1:1000
Vinculin	abcam, ab129002 Sigma hVIN-1	Rabbit Mouse	1:1000
Total ATM	abcam, ab32420	Rabbit	1:1000
Total ATR	Cell Signaling 2790	Rabbit	1:1000
AR NTD	Dako clone 441	Mouse	1:1000
ARv7	RevMab RM7	Rabbit	1:1000
cMyc	Santa Cruz 9E10 sc-40		
PTEN	Cell signaling D4-3 9188	Rabbit	1:1000
p53	Dako DO-7	Mouse	1:5000
pKAP	Cell signaling 5868	Mouse	1:1000
PSA	Dako A0562	Rabbit	1:1000
Secondary antibody			
IgG (H+L) Cross-Adsorbed Goat anti-mouse, Alexa Fluor 488, Invitrogen. Fisher Scientific 10256302			1:5000
IgG (H+L) Cross-Adsorbed Goat anti-Rabbit, Alexa Fluor 568, Invitrogen. Fisher Scientific 10463022			1:5000

NTD, N-terminal domain, CTD C-terminal Domain

Supplementary Table 5: Patient characteristics

Characteristic	ATM loss	Control cohort
n	60	88
Age at diagnosis, years (IQR)	62.0 (55.0-66.0)	60.5 (56.8-66.0)
Histology (%) Adenocarcinoma Adenocarcinoma with neuroendocrine features Unknown	56 (92) 2 (3.3) 3 (4.9)	81 (92) 0 (0.0) 7 (8.0)
Total Gleason score (IQR)	9.0 (7.0-9.0)	9.0 (7.0-9.0)
PSA at diagnosis (median,IQR)	97.2 (23.3- 342.0)	75.4 (26.8 - 220.5)
Baseline TNM stage		
T (%) 1 2 3 4 Unknown	0 (0.0) 5 (8.2) 24 (39) 15 (25) 17 (28)	2 (2.3) 5 (5.7) 37 (42) 11 (13) 33 (38)
N (%) 0 1 2 Unknown	11 (18) 28 (46) 1 (1.6) 21 (34)	27 (31) 20 (23) 1 (1.1) 40 (46)
M (%) 0 1 Unknown	13 (21) 42 (69) 6 (9.8)	36 (41) 37 (42) 15 (17)
Radical treatment given upfront (%)	13 (21)	37 (42)
Prior treatments Novel hormonal therapy (abiratarone/enzalutamide) Docetaxel	61 (100) 57 (93)	88 (100) 83 (94)

Supplementary Table 6. Detailed information of patients IHC and sequencing results (separate excel file)

Supplementary Table 7. ATM CRISPR clones sequences

Clone	Alelle	cDNA	Protein
WT1		ATM wt	ATM wt
WT2		ATM wt	ATM wt
CL1	1	c.3378_3379ins(275)	p.Lys1126insTer10
	2	c.3369_3380del	p.Tyr1124_Ala1127del
CL2	1	c.3376_3383del	p.Lys1126GlyfsTer7
	2	c.3368_3369ins(278)	p.Ala1123insTer37
	3	c.3342_3363del	p.Leu1115MetfsTer3
CL3	1	c.3355_3356ins(460)	p.Phe1120insTer4
	2	c.3355_3356ins(460)	p.Phe1120insTer4
CL4	1	c.3341_3342ins(206)	p.Lys1114insTer43
	2	c.3378_3379insAGCTTTTGGT,c.3379_3398del	p.Ala1127SerfsTer4
CL5	1	c.3339_3340insGAATG	p.Leu1113insGluTer
	2	c.3332_3402del	p.Pro1112_Met1134del, p.Ser1135ProfsTer
CL6	1	c.3356_3357ins(22)	p.Asn1122insTer5
	2	c.3355_3356ins(154)	p.Ala1123insTer11
CL7	1	c.3378_3379ins(104)	p.Lys1126InsTer3
	2	c.3364_3365(210)	p.Glu1121InsTer1
CL8	1	c.3346_3347ins(242)	p.Leu1115insTer9
	2	c.3301_3388del	p.Lys1101GlufsTer
		wt	
		In-frame	
		Truncating	

3. Supplementary Figures

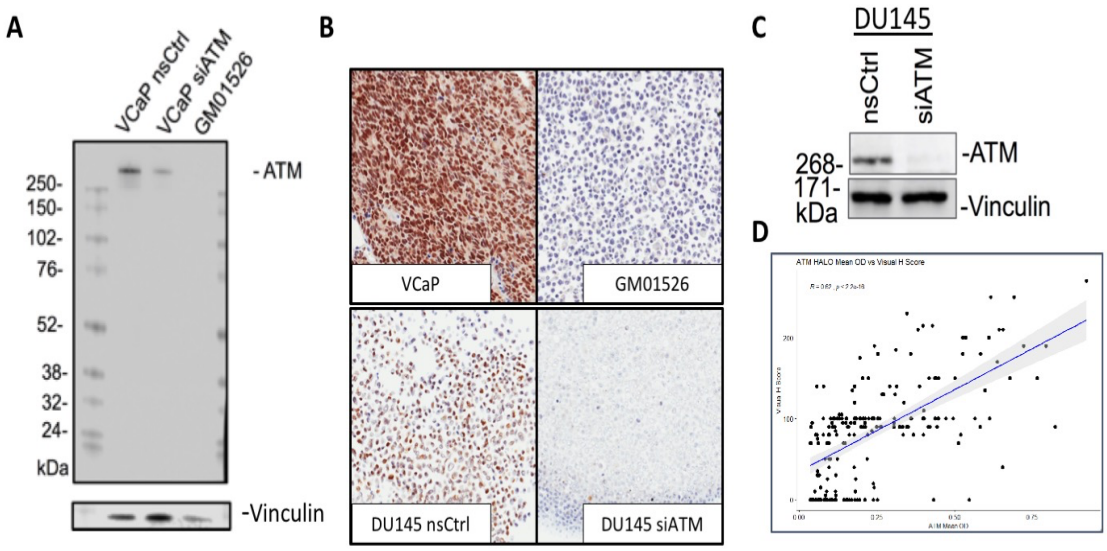

Supplementary Figure 1: Validation of the ATM antibody for IHC. A) The ATM positive cell line VCAP was treated with either control or ATM siRNA and protein lysate run for western blot analysis. The ATM negative cell line GM01526 was used as negative control. **B/C)** Additionally, IHC was run on VCAP, GM01626, and siRNA ATM treated DU145 cells to ensure antibody specificity. **D)** Visual H-score by a pathologist was correlated to the digital, artificial intelligence trained Halo score to validate reproducibility of the IHC results.

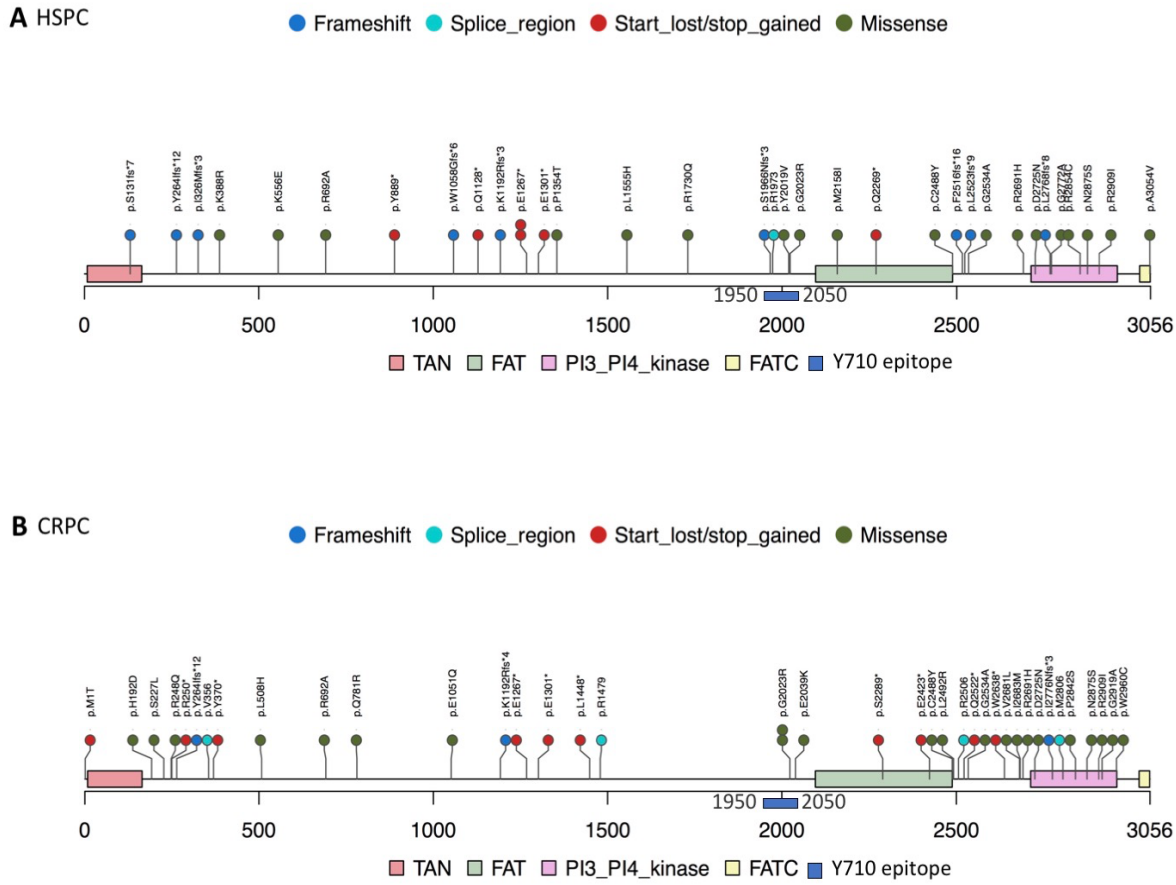

Supplementary Figure 2: Genomic characterization of ATM mutations separated by prostate cancer stage. Lollipop charts showing the location and type of mutations found across the ATM gene in the study population, divided by sample type **A)** hormone sensitive (HSPC) and **B)** castration resistant state (CRPC) biopsies.

Supplementary Figure 3

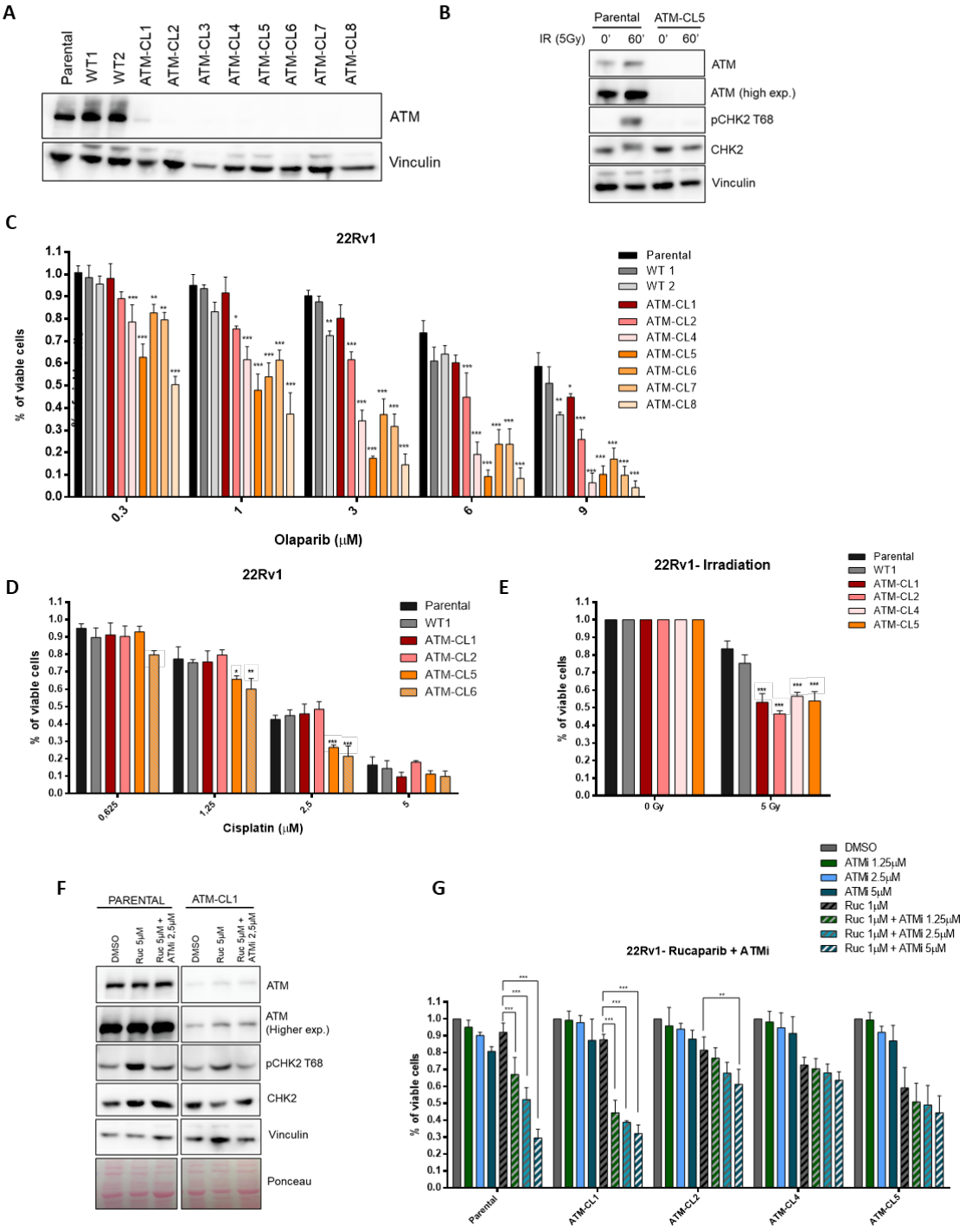

Supplementary Figure 3. ATM loss in 22Rv1 CRISPR clones alters response to PARPi, Cisplatin and Irradiation. A) Western-blot images for ATM expression for the 22Rv1 CRISPR clones. **B)** Western-blot image showing absence of Chk2 T68 phosphorylation induction after irradiation (5Gy) in the ATM-CL5. Vinculin and total

Chk2 were blotted as normalizers. **C-D**) 22Rv1 cell line models were treated for 6 days with the indicated doses of Olaparib (n=3) (C) and Cisplatin (n=4) (D). Cell viability was estimated based on percentage of cells negative for both Annexin V and PI staining. **E)** Indicated 22Rv1 cell line models were irradiated with 5Gy (n=3)**,** cell viability was assessed 6 days after irradiation based on percentage of cells negative for both Annexin V and PI staining. **F-G)** ATM-CL1 retains expression of a functional ATM protein that correlates with no sensitivity to PARPi **(F)** Western-blot images showing that ATM-CL1 retains ATM expression and ATM-dependent induction of pChk2 T68 **G)** 22Rv1 cell line models were treated for 6 days with the indicated doses of Rucaparib and ATMi (KU-60019) (n=4). Opposite to ATM CRISPR models with complete loss of ATM, ATM-CL1 was highly sensitive to ATM inhibition further indicating that this clone retains some ATM function. Cell viability was estimated based on percentage of cells negative for both Annexin V and PI staining. All statistical significances were calculated using one-way ANOVA, *** $P < 0.001$; ** $P < 0.005$; *$P < 0.05$. All error bars represent means ± s.d. n represents number of independent experiments.

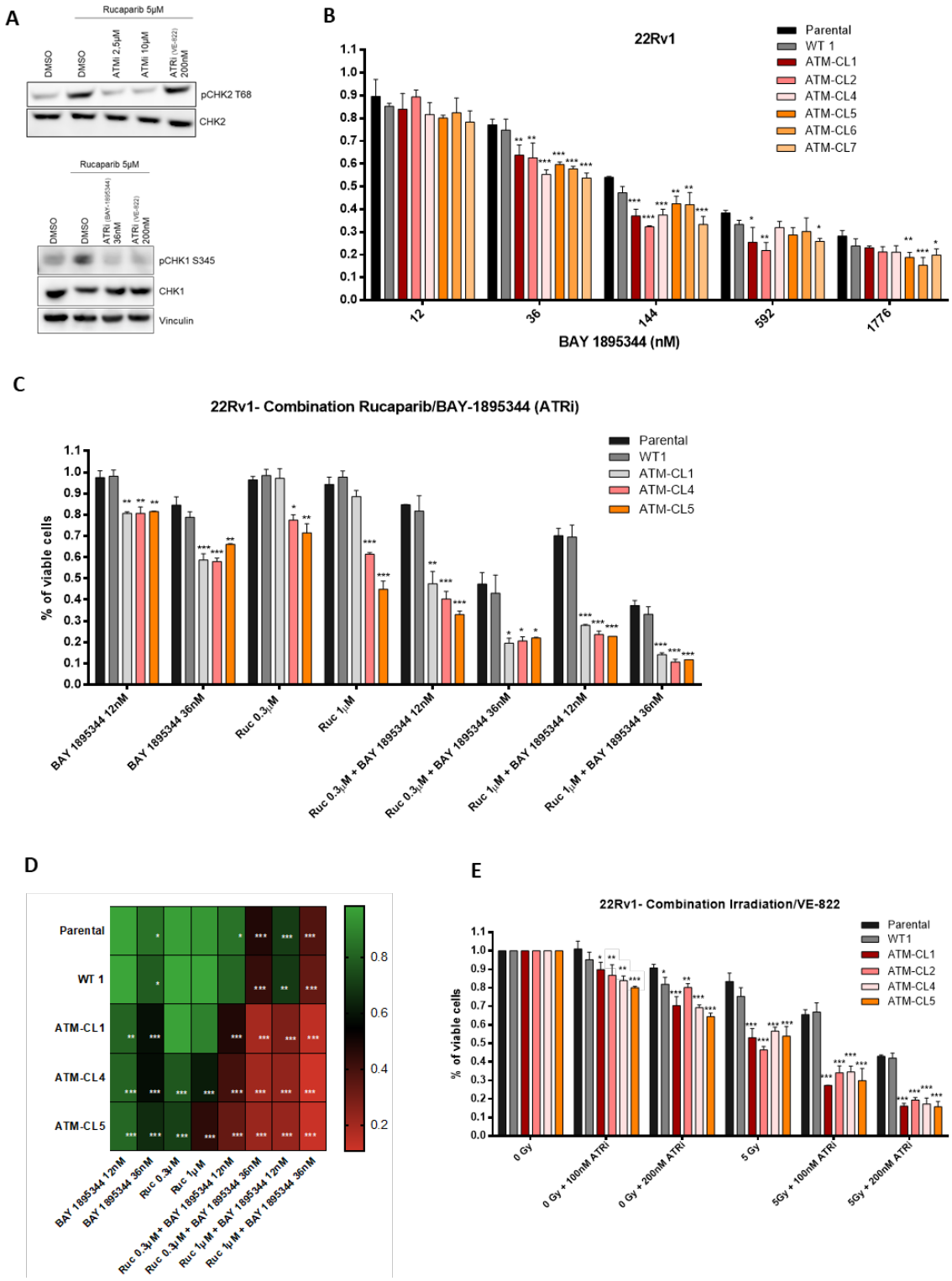

Supplementary Figure 4. Enhanced sensitivity of ATM-deficient models to dual PARP-ATR inhibition is also observed when using the ATRi BAY-1895344. A) (upper panel) ATM (KU-60019) suppressed CHK2 phosphorylation (T68) and (bottom panel) ATR inhibitors (VE-822 and BAY-1895344) suppressed CHK1 phosphorylation (S345)

B-C) Indicated 22Rv1 cell line models were treated for 6 days with the specified doses of BAY-1893544 (n=3) (B) or the indicated combinations of Rucaparib and BAY-1895344. Statistical tests compared each clone to the parental cell line. **D)** Heat maps depicting enhanced sensitivity of ATM-deficient models to dual PARP (Rucaparib)-ATR (BAY-1895344) inhibition. Statistical tests compare each clone to their untreated condition (n=2). **E)** Untreated or irradiated (5Gy) 22Rv.1 cells line models were treated with the indicated doses of ATRi (VE-822) (n=3). Statistical tests compared each clone to the parental cell line. In all panels cell viability was estimated based on percentage of cells negative for both Annexin V and PI staining. All Statistical significances were calculated using one-way ANOVA, *** $p \leq 0.001$; ** $p \leq 0.005$; * $p \leq 0.05$. All error bars represent means ± s.d. n represents number of independent experiments.

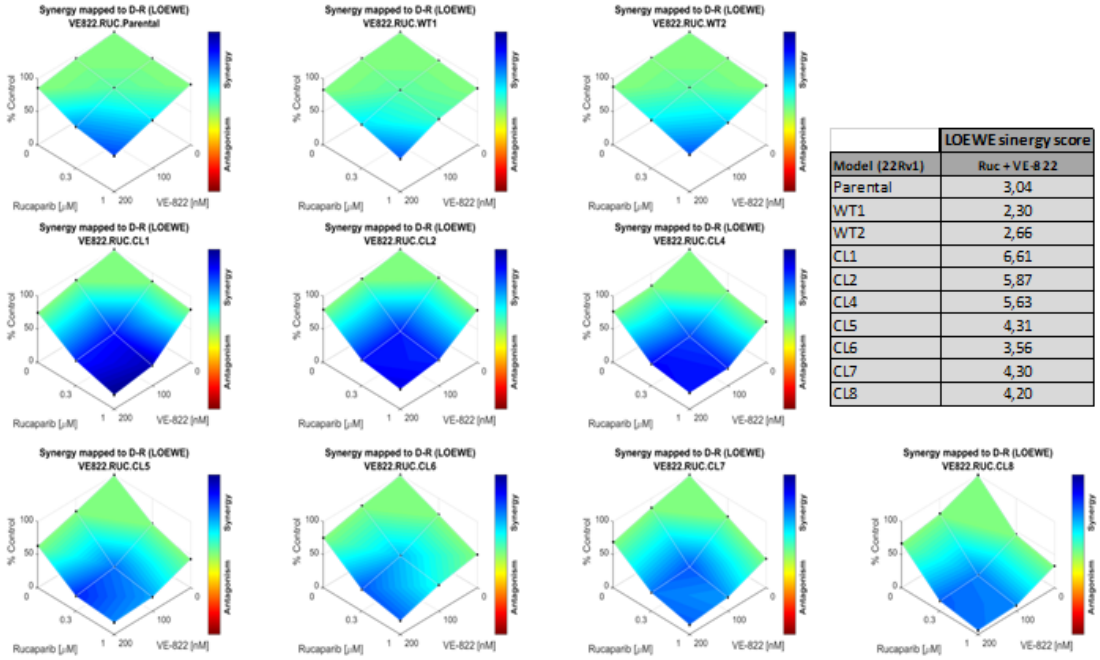

	LOEWE sinergy score
Model (22Rv1)	Ruc + VE-822
Parental	3,04
WT1	2,30
WT2	2,66
CL1	6,61
CL2	5,87
CL4	5,63
CL5	4,31
CL6	3,56
CL7	4,30
CL8	4,20

Supplementary Figure 5. Graphical representation of synergistic interaction using the Loewe model [De Veroli et al, Bionf 2016; 32(18)2866-2868] for different doses of the ATR inhibitor VE-822 and the PARP inhibitor rucaparib when treating 22Rv1 parental, ATMwt or ATM CRISPR clones. Drug concentrations are represented in the X axis, and the Y axis represents percentage of viable cells.

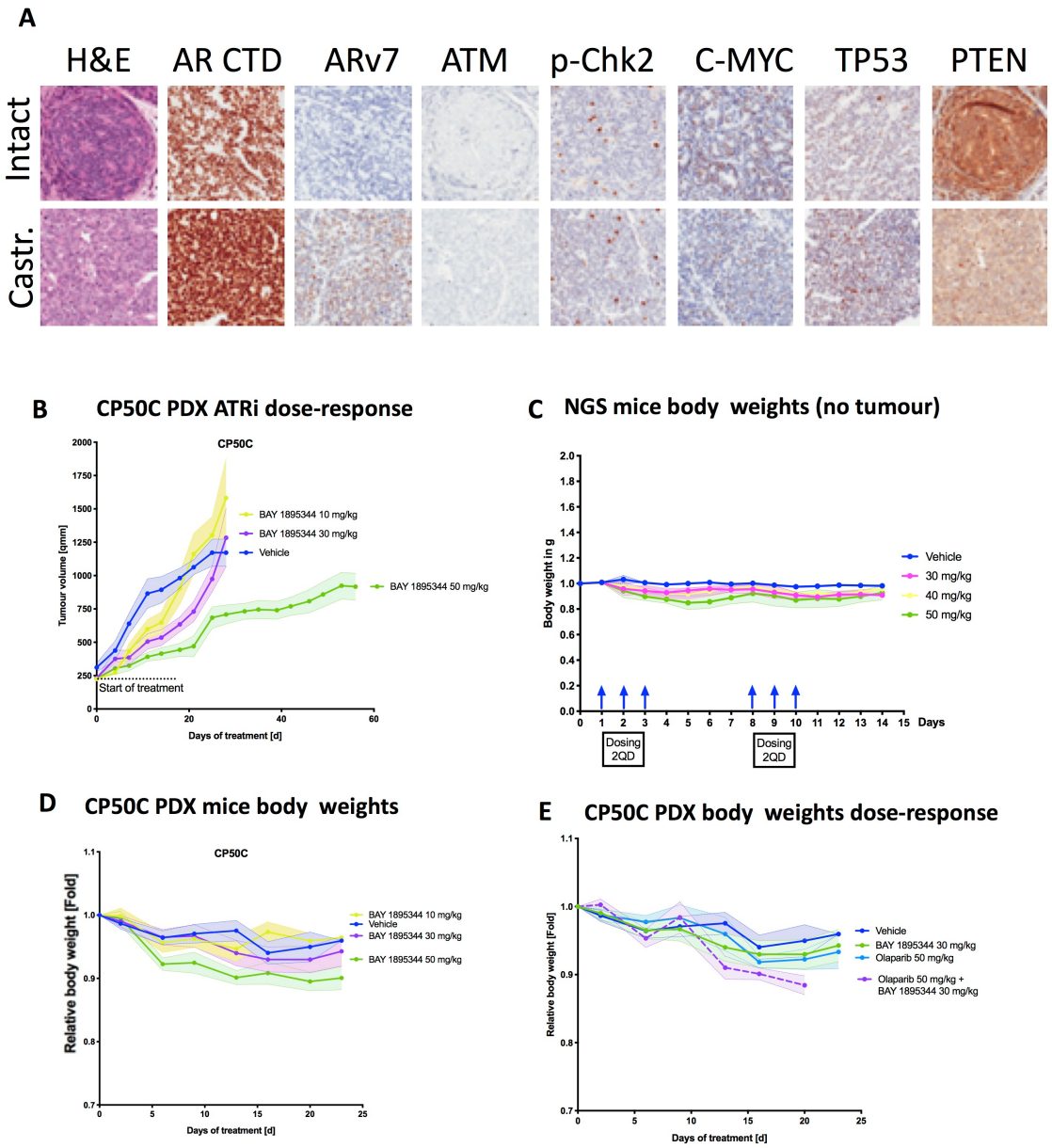

Supplementary Figure 6: Dose toxicity test for BAY 1895344. A) Expression of different markers in castrated and intact PDX tumour mice, analysed by IHC. **B-E)** Castrated mice growing the patient derived tumour model CP50 were treated as soon as the tumours reached a volume of 200 mm^3 with the ATR inhibitor BAY1895344 (10, 30, 50 mg/kg 2QD, - days on, 4- days off). Tumours were measured twice-weekly using calipers **(B)** and body weight was monitored twice-weekly for the dose tolerance test **(D)** as well as for the experiments presented in the main Figure 5 where the medium dose (30mg/kg) of BAY 1895344 was compared to and combined with treatment with the

PARP inhibitor Olaparib (50 mg/kg, i.p, QD in 10% 2-HPbCD/PBS) **(E)**. Dose toxicity of three different doses (30, 40, 50 mg/kg 2QD, 3-days on, 4-days off) of the ATR inhibitor BAY 1895344 was tested on non-tumour bearing NSG NOD scid gamma mice (n= 3) over a period of two weeks **(C)**. Body weight was taken daily. Error shadows represent standard error, Group size per arm is n=8. All statistical tests are calculated against vehicle control using students t-Test, *** $p \leq 0.001$; ** $p \leq 0.005$; * $p \leq 0.05$.

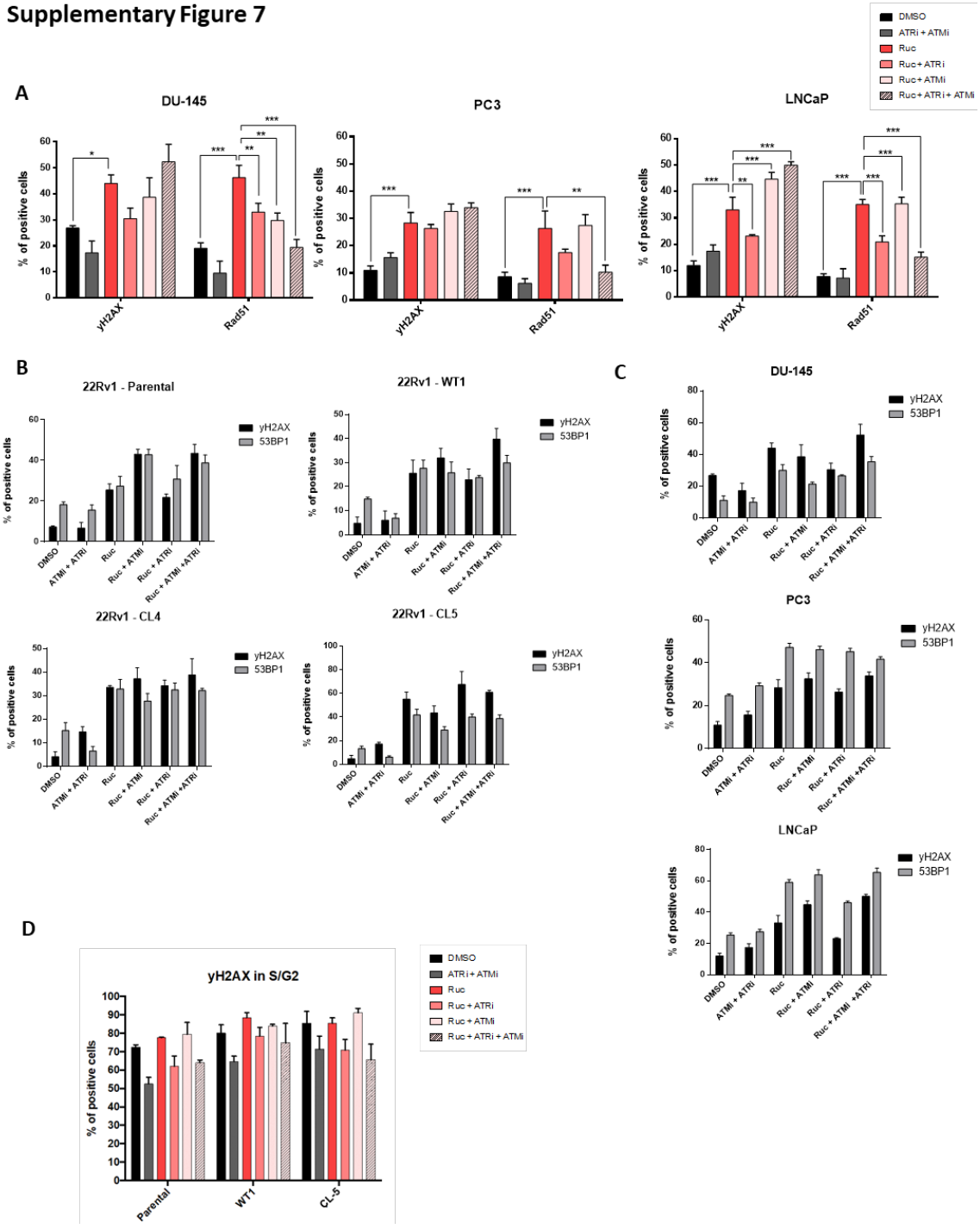

Supplementary Figure 7. HRR suppression after ATM and ATR inhibition in PARPi-treated cells is conserved across different prostate cancer cell lines. A) Quantification of the percentage of cells positive (>5 foci) for γH2AX and RAD51 (n=3) by immunofluorescence staining in PC3, DU145 and LNCaP parental cell lines after

treatment with 1μM of rucaparib alone, or in combination with 2.5μM of the ATMi (KU-60019), and/or 200nM of the ATRi (VE-822) for 24-hours. Statistical comparisons are calculated using one-way ANOVA; *** $P < 0.001$; ** $P < 0.005$; *$P < 0.05$. All error bars represent means ± s.d.; n represents number of independent experiments. **B-C)** Assessment of DNA damage by quantification of the percentage of cells positive (>5 foci) for γH2AX and 53BP1 (n=3) by immunofluorescence staining in **(b)** 22Rv1 parental cells and ATMwt (WT1) and ATMko (CL4,CL5) clones and in **(c)** PC3, DU145 and LNCaP parental cell lines. Cells were treated with 1μM of Rucaparib alone or in combination with 2.5μM of the ATMi (KU-60019) and/or 200nM of the ATRi (VE-822) for 24 hours. All error bars represent means ± s.d. n represents number of independent experiments.

D) Sensitivity to PARPi is not the result of impaired cell recognition of DNA damage and ability to progress to S/G2. Cells were treated with 1μM of rucaparib alone, or in combination with 2.5μM of the ATMi (KU-60019), and/or 200nM of the ATRi (VE-822) for 24-hours ; γH2AX was used as a marker of damage, and geminin as a marker of the S/G2 phase of the cell cycle ; positive co-staining was analyzed by immunofluorescence and quantified. Plots represent the percentage of cells positive for both yH2AX (>5 foci) and geminin (intensity) in 22Rv1 parental cells and ATMwt (WT1), and ATMko (CL5) clones (n=2). All error bars represent means ± s.d. n represents number of independent experiments.

4. Supplementary references

1. Balmus G, Pilger D, Coates J, et al. ATM orchestrates the DNA-damage response to counter toxic non-homologous end-joining at broken replication forks. *Nature communications.* 2019;10(1):87.
2. Drost J, Karthaus WR, Gao D, et al. Organoid culture systems for prostate epithelial and cancer tissue. *Nature protocols.* 2016;11(2):347-358.